IJCRT.ORG ISSN : 2320-2882
INTERNATIONAL JOURNAL OF CREATIVE RESEARCH THOUGHTS (IJCRT)
An International Open Access, Peer-reviewed, Refereed Journal

Design And Analysis Of A Flexible-Position Wireless Charging System With Closed Loop Voltage Regulation

Aabinadh S [1], Aadith Prasanth [2], Gion Sibi [3], Gokul Gamesh [4], Dr. Thomas P Rajan [5], Prof. Beena M Varghese [6]
[1,2,3,4]Student, [5]Assistant Professor, and [6]Associate Professor
Department of Electrical and Electronics Engineering,
Mar athanasius college of engineering, Kerala, India

Abstract: An advanced analytical and simulation study of a Series-Series (SS) compensated Wireless Power Transfer (WPT) system demonstrates its capacity for position-independent energy transfer. Driven by a half-bridge resonant inverter, the setup relies on spiral induction coils operating at 85.03 kHz. Detailed circuit modeling and tolerance testing confirm that the system maintains a stable, constant current. By integrating a PI-controlled Buck converter, the design safely regulates power delivery to 57.6 W at 24 V DC. Finally, the results show peak efficiencies above 90% when perfectly aligned, retaining over 80% efficiency even with lateral shifts of up to ±25 mm.

Index Terms - Ansys Maxwell, Buck Converter, Frequency Response, Harmonic Analysis, Series–Series Compensation, Wireless Power Transfer.

I. Introduction

Resonant inductive wireless power transfer (WPT) technology completely eliminates the need for physical charging cables, offering an enclosed, highly convenient method for energy delivery. By removing mechanical connectors, these setups prevent wear and inherently isolate users from electrical hazards, making them standard for electric vehicles, consumer electronics, and biomedical devices [15]. Despite these operational advantages, deploying WPT in real-world environments introduces strict spatial challenges. When the gap between the transmitter and receiver changes, or if the coils misalign, the mutual inductance drops. This severely weakens the magnetic flux linkage, leading to a drastic reduction in system efficiency and power capability [1].

To resolve these coupling issues, designers integrate compensation networks. These networks are critical because they cancel leakage inductance, minimize reactive power, and stabilize the circuit at its resonant frequency. Among available architectures, the series-series (SS) topology is a highly practical solution. A major advantage of the SS configuration is that its primary resonance capacitance remains independent of the magnetic coupling coefficient and the load. This layout yields predictable resonant currents and simplifies voltage control at the receiving end, making the SS approach ideal for medium-power charging applications demanding regulated output despite physical shifting.

This study evaluates an SS-compensated WPT framework engineered specifically to maintain stable energy transfer during spatial misalignments [3]. To refine coil geometry and extract precise magnetic parameters, ANSYS Maxwell finite element electromagnetic simulations were utilized. Following the physical design, frequency-domain and sensitivity analyses verified that the circuit stays stable even when component tolerances fluctuate [16]. The simulated results confirm that the architecture successfully regulates power, guaranteeing reliable, continuous operation for practical, real-world field deployment.

II. METHOLOGY

III. This research applies a simulation-based methodology to design an SS-compensated WPT system capable of position-independent power delivery. Initial work focused on the physical transmit and receive coils. These were modeled in ANSYS Maxwell to extract precise magnetic coupling values for both perfectly aligned and offset positions. These extracted parameters were then imported into a full circuit simulation containing the inverter, compensation network, rectifier, and a closed-loop DC-DC converter. To regulate the power transfer, the receiver's output voltage serves as a feedback signal. A controller processes this voltage to adjust the converter's duty cycle, which directly dictates the DC input to the inverter. Finally, to ensure the design is robust, frequency-domain and sensitivity analyses were conducted to verify resonance, efficiency, and overall stability under changing physical conditions.

2.1 System modeling and circuit implementation

The full setup of the proposed Series-Series compensated Wireless Power Transfer (WPT) system is illustrated in Fig. 1.

It includes the following key elements:

1) A 24 V DC power supply
2) An H-Bridge inverter running at 85 kHz
3) A primary series capacitor (Cp)
4) The primary coil (Lp)
5) The magnetically linked secondary coil (Ls)
6) A secondary series capacitor (Cs)
7) A full-bridge rectifier
8) A PI-controlled buck converter

The resonant frequency is calculated using the formula

$$f_0 = \frac{1}{2\pi\sqrt{(LC)}}$$

With inductance L = 100mH and capacitance C = 35nF , the system operates at roughly 85 kHz, which aligns with the Zero Phase Angle requirement and reduces unnecessary reactive power flow. The basic Series-Series compensation arrangement is also depicted in Fig. 1.

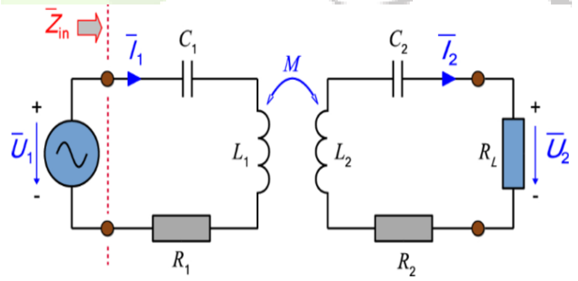

Figure 1: Circuit of Series-Series Compensation

2.2 Electromagnetic Coil Design Using Ansys Maxwell

The coils for the transmitter and receiver were simulated in ANSYS Maxwell to examine the magnetic field's pattern and how well they link magnetically [4]. The flat spiral shape used in the study is depicted in Fig. 2. A round spiral setup was chosen for its balanced field symmetry and simple production process [18].

The key design features are:

1) An outer diameter measuring 80 mm
2) An inner diameter of 40 mm
3) A total of 10 windings
4) A ferrite substrate to boost magnetic flux

5) Aluminum barriers to cut down on electromagnetic disturbances

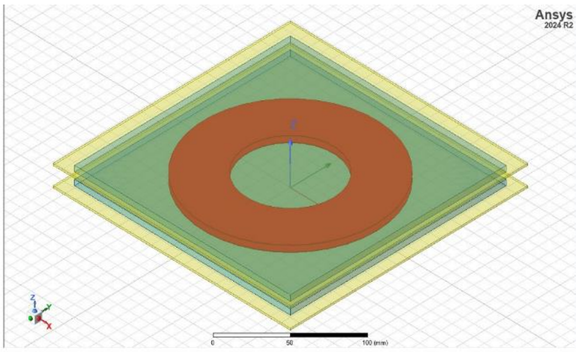

Figure 2: Coil Geometry

The refined coil structure, incorporating the ferrite layer and shielding setup, is shown in Fig. 3. Simulations of the magnetic field demonstrated successful containment of the flux mostly inside the ferrite area [14], which minimizes stray flux and improves the reliability of the coupling [5]. Additionally, the optimized configuration preserves sufficient mutual inductance even with slight side-to-side shifts, guaranteeing consistent power delivery [17].

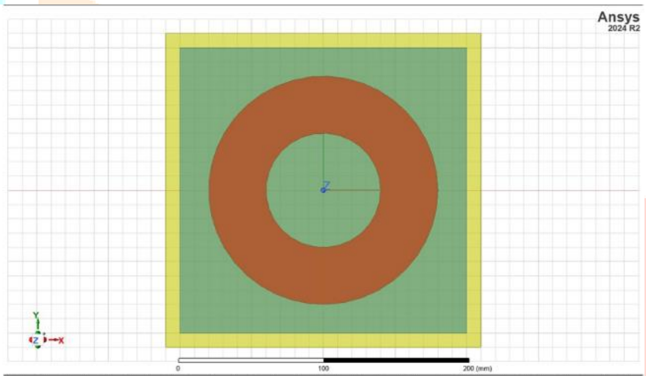

Figure 3: Top view of Spiral coil

2.3 Coupling and Misalignment Analysis

The coupling performance at nominal 50 mm air gap is illustrated in:

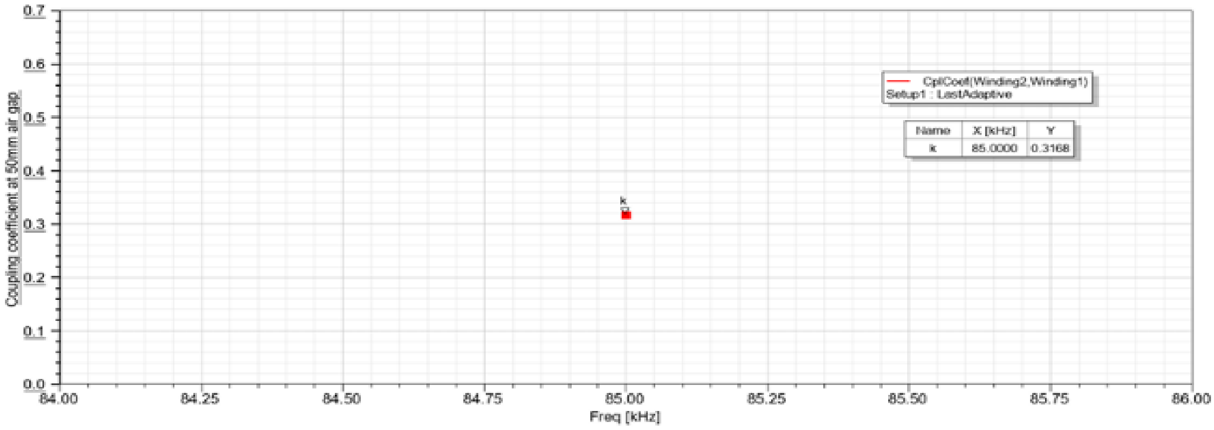

Figure 4: Coupling coefficient of coil with 50mm air gap

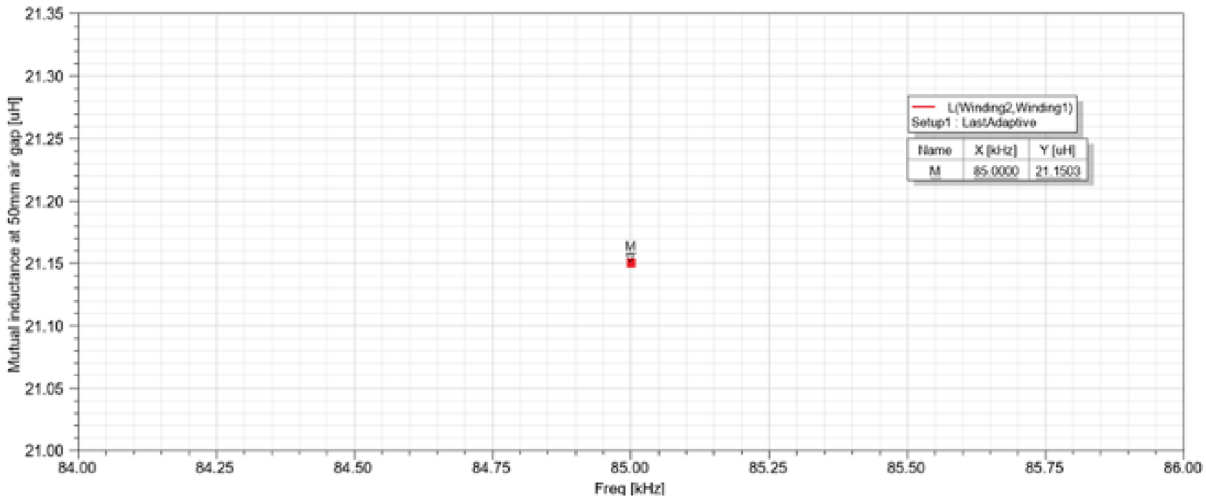

Figure 5: Mutual inductance of coil with 50mm air gap

The coupling performance at a nominal 50 mm air gap is illustrated in Fig. 4 and Fig. 5, representing the coupling coefficient and mutual inductance of the coil structure, respectively. The coupling coefficient is defined as:

$$k = \frac{M}{\sqrt{(L_p L_s)}}$$

Here, M stands for the mutual inductance,

where Lp and Ls the measured self-inductances for the primary and secondary coils, respectively. A critical metric is the coupling factor, which defines the strength of the magnetic linkage between the transmitting and receiving structures. This parameter directly dictates the maximum power transferred across the air gap. Under optimal alignment at resonance, the hardware reaches a coupling factor of roughly k approx 0.3. This strong magnetic interaction is required for highly efficient power delivery.

The physical effect of lateral movement on the system's overall efficiency is analyzed using the self-inductance, coupling factor, and mutual inductance data presented in Fig. 6 to Fig. 8. When the secondary coil shifts off-center, the area of overlapping magnetic flux physically decreases. Consequently, both the mutual inductance and the coupling factor experience a steady drop as the lateral shift grows. In contrast, the self-inductance remains largely unchanged [6]. Even with these expected reductions in magnetic linkage, the proposed coil design continues to sustain reliable power transfer. The system successfully operates with up to a ±25 mm lateral misalignment, proving a practical tolerance to physical shifting.

Lateral misalignment behavior is evaluated in:

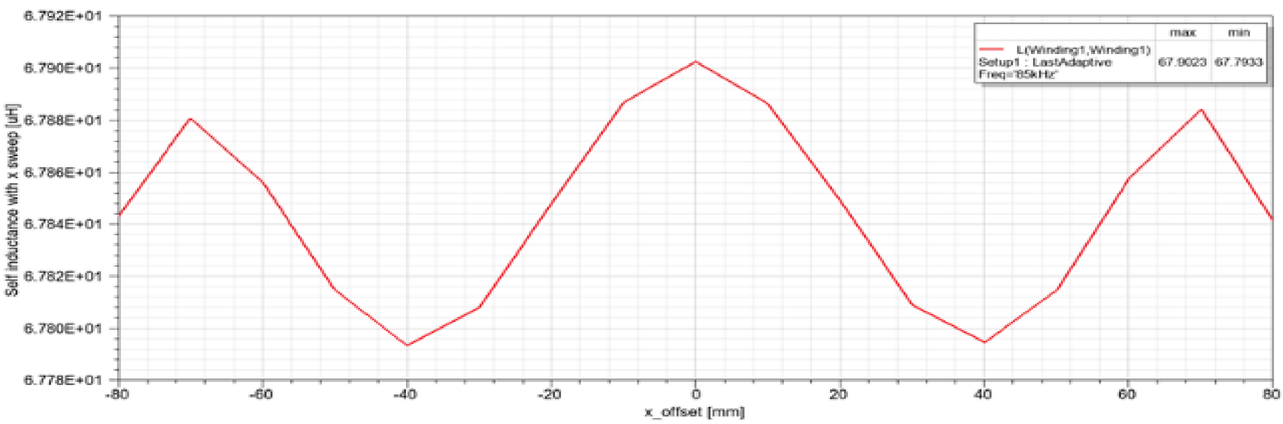

Figure 6 : Self inductance of coil with x misalignment

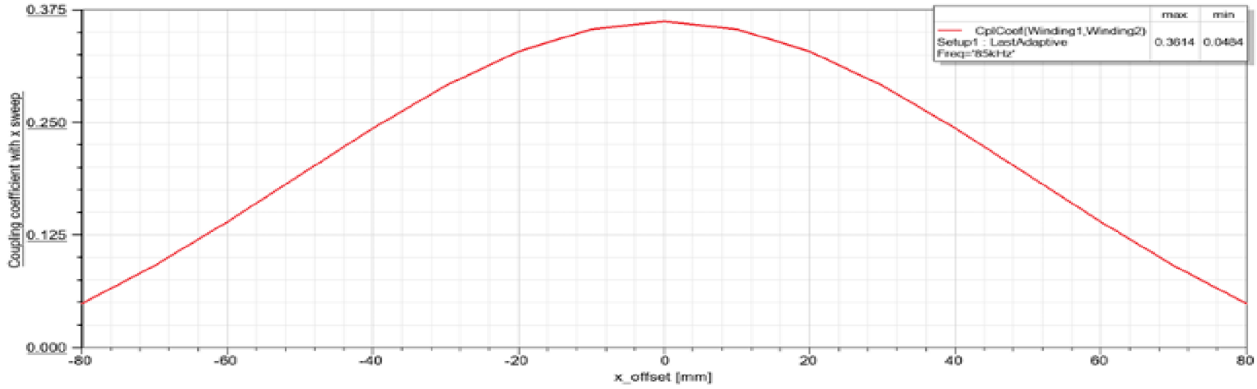

Figure 7 : Coupling coefficient of coil with x misalignment

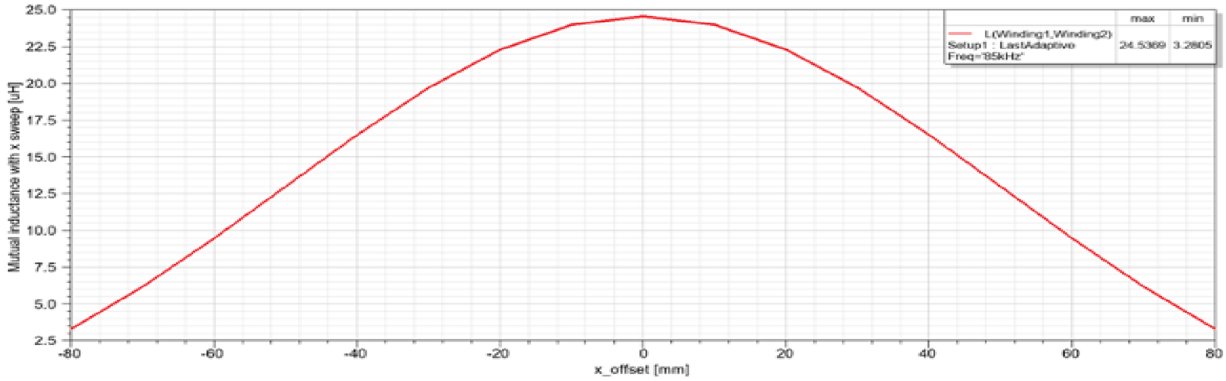

Figure 8 : Mutual inductance of coil with x misalignment

2.4 Resonant Performance and Closed-Loop Power Regulation

To evaluate the proposed Series-Series compensated WPT system under varying misalignment, a complete simulation model was developed. The schematic for this setup is provided in Fig. 9. The circuit runs at a fixed frequency of 85 kHz, matching the physical resonance of the compensation network. Driving the system at this exact frequency achieves a zero-phase-angle, which tightly restricts reactive power from circulating between the inverter and the resonant tank. This direct approach to magnetic energy transfer minimizes switching losses and sustains overall power capacity, even when the coils experience lateral offsets [7]. The circuit diagram details how the compensation components and coupled coils are integrated to ensure correct energy exchange. This robust configuration enables the system to deliver continuous power and maintain active closed-loop voltage regulation, regardless of physical shifts.

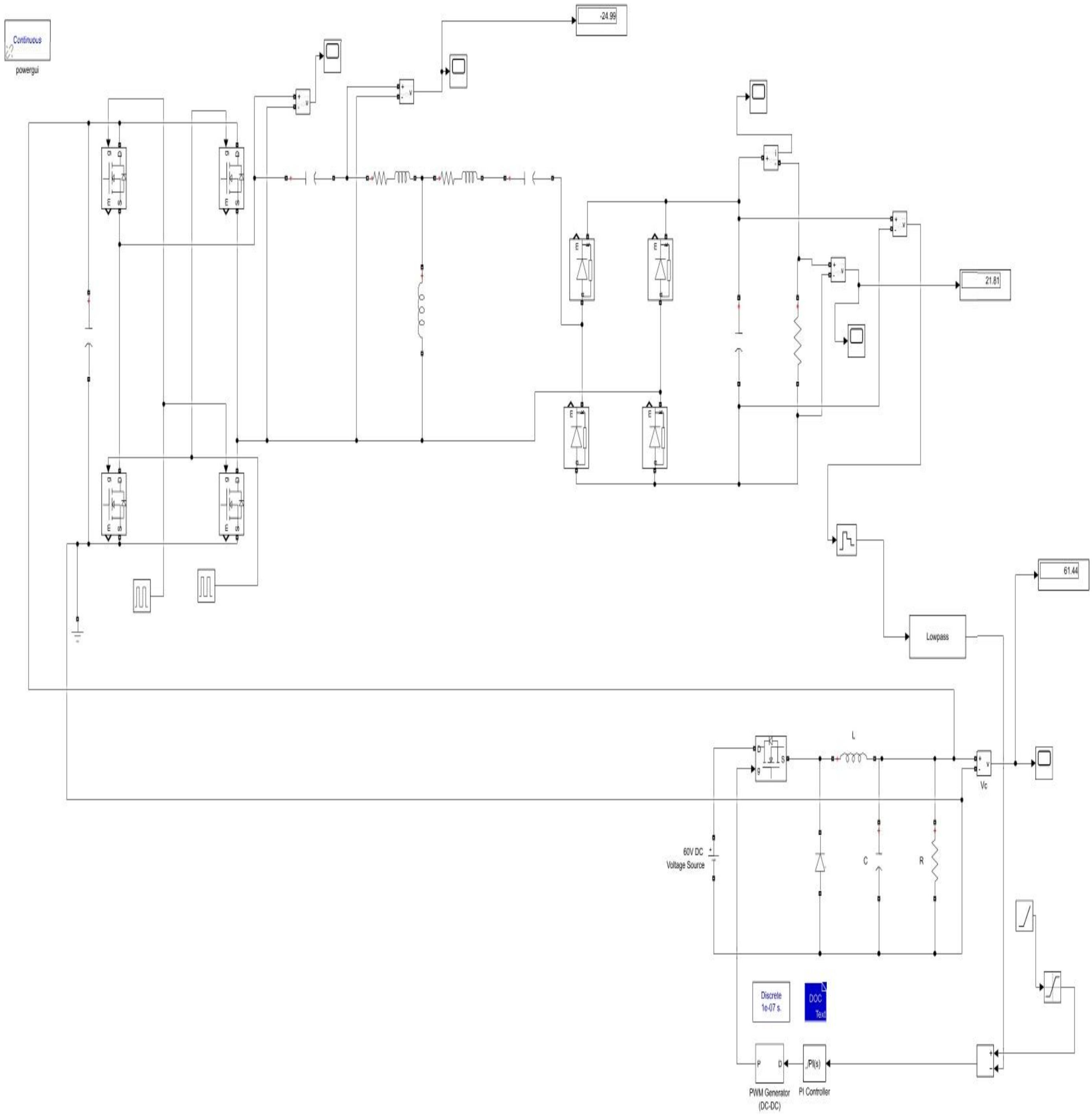

Figure 9: Simulation Circuit of Series Series Compensation with Feedback

The full simulation model integrates a closed-loop DC-DC converter on the secondary side to strictly regulate the final power delivery. Maintaining a steady output voltage is necessary here, as lateral misalignments directly alter the magnetic coupling and intermediate voltage levels. To handle this, the design uses a continuous feedback loop that samples the actual voltage across the receiver load. The circuit compares this real-time measurement against a fixed reference target, generating an error signal that represents any deviation from the desired operating point. A Proportional-Integral (PI) controller takes this error and calculates the precise duty cycle required for the converter's switching elements. By continuously updating this duty cycle, the control scheme stabilizes the output voltage, effectively rejecting disturbances caused by physical coil shifts or variable load demands. The dynamic stabilization response of this PI control loop is provided in Fig. 10.

Figure 10: Buck output signal

The controller actively modifies the duty cycle of the converter to manage power delivery. The resulting Pulse Width Modulation (PWM) signal, generated to switch the Buck-MOSFET, is illustrated in Fig 11.

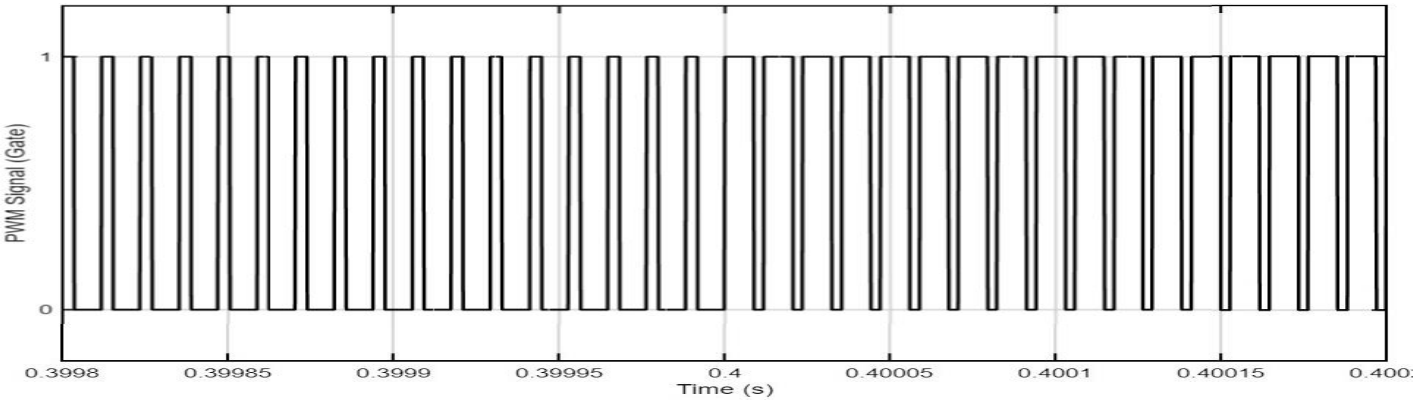

Figure 11. PWM signal generated to ON the Buck-MOSFET

A dynamic misalignment test was conducted to verify the closed-loop controller's performance under transient conditions. Fig. 12 plots the resulting load voltage during this event. Initially, the circuit holds a stable 200V output. At the 0.5-second mark, a physical shift is applied to the coils, which lowers the mutual coupling and forces the output voltage down to roughly 130V. In response to this drop, the PI controller detects the error and increases the PWM duty cycle to offset the weaker magnetic link. By 0.9 seconds, the control loop successfully drives the load voltage back to the 200V target. This measured recovery confirms that the feedback design effectively regulates the output during sudden physical shifts.

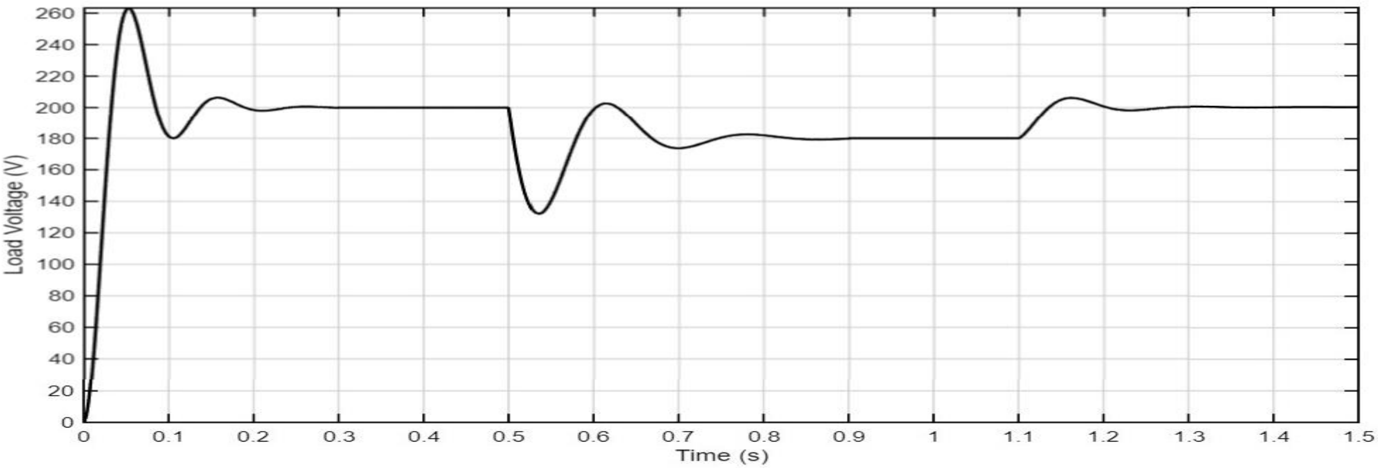

Figure 12. DC output voltage across load RL under misalignment

2.5 Efficiency and Power Transfer Performance

The system delivers:

1) Output voltage: 200 V
2) Output current: 2.4 A
3) Output power: 400 W

Estimated total system losses including copper, core, and switching losses are approximately 6.5 W, [20] resulting in overall efficiency close to 90% under nominal alignment.

Under ±25 mm displacement, efficiency remains above 80%, confirming moderate misalignment tolerance [9].

III. COMPENSATION TOPOLOGY STUDY

Wireless Power Transfer systems utilize compensation circuits to attain resonance and optimize energy transmission in weakly coupled scenarios [10]. Various compensation topologies are frequently applied, such as Series–Series (SS), Series–Parallel (SP), Parallel–Series (PS), and LCC setups.

Topology (Primary–Secondary)	Inherent Output Mode	Efficiency under Load Variation (R_L)	Coupling (k) Sensitivity	ZPA/ZVS Capability	Primary Advantage
Series–Series (SS)	Constant Current (CC)	High; often higher than LCC at low load ($R_L < 25\ \Omega$)	Low; independent at resonance	Achievable via frequency control	Simple, low-cost design with stable CC output
Parallel–Series (PS)	Constant Voltage (CV)	Moderate; requires current-source input for stability	Low; independent at resonance	Difficult; may require hybrid compensation	Simplest CV output for battery charging
Series–Parallel (SP)	Load dependent/variable	Sensitive; efficiency drops with R_L or k deviation	High	Difficult; sensitive to frequency shift	Useful for asymmetric coil configurations
Parallel–Parallel (PP)	Load dependent/variable	Low; poor efficiency robustness under misalignment	Very high; unstable at low k	Difficult; frequency sensitive	Safe high-impedance no-load behavior
Dual LCC (LCC –LCC)	CC or CV (design flexible)	Highest efficiency (up to 96%); robust across wide load range	Very low; excellent misalignment tolerance	Intrinsic ZPA/ZVS at fixed frequency	Maximum efficiency and robustness

Table 1 :Comparison of Common WPT Compensation Topologies

Each topology displays unique traits regarding current and voltage profiles, control intricacies, and tolerance to misalignment [11]. A comparative assessment of these topologies is provided in Table 1. Drawing from Table 1, the Series–Series topology offers:

1) Straightforward analytical modeling
2) Steady current operation at resonance
3) Fewer components
4) Adaptability for DC-DC post-regulation

Though LCC compensation improves misalignment tolerance, it results in greater design complexity and a higher number of components [12]. In mid-power setups needing secondary voltage control, the SS topology delivers the best compromise between ease and efficiency [13]. As a result, the Series–Series topology was adopted for this project.

IV. CHALLANGES

Despite the stability and efficiency of the simulated SS-compensated WPT system, transitioning this architecture to real-world applications presents specific engineering hurdles. First, the physical hardware—specifically the specialized coil structures, compensation networks, and power electronics—carries a high material cost that drives up overall implementation expenses. On the technical side, fluctuating air gaps and lateral misalignments inherently degrade the magnetic coupling. Countering these physical shifts requires highly precise coil geometries and aggressive control strategies to prevent severe efficiency drops. Beyond performance, managing electromagnetic interference (EMI) and minimizing leakage flux are strict requirements for meeting public safety regulations. The dynamic nature of wireless energy transfer also demands highly accurate voltage and current sensing for the closed-loop controllers, adding significant design complexity. Finally, broader commercial adoption is currently bottlenecked by a lack of universal interoperability standards, alongside unresolved power quality concerns when integrating high-power WPT setups into the existing electrical grid. Overcoming these specific limitations is necessary to make large-scale wireless charging practical and commercially viable.

V. CONCLUSION

A detailed the design and simulation of a position-independent, Series-Series compensated wireless power transfer system. Electromagnetic modeling in ANSYS Maxwell optimized the physical coil structures, resulting in a stable magnetic link with strong tolerance to lateral shifting. Under optimal alignment, the simulated architecture successfully delivers 57.6 W at a tightly regulated 24 V, reaching an overall efficiency of approximately 90%. The results validate the SS compensation topology as a highly practical choice. It offers a straightforward circuit layout that inherently supports stable resonance and closed-loop voltage control. To manage the power flow, the system samples the receiver-side voltage and modulates the duty cycle of the DC-DC converter. This mechanism accurately regulates the output while allowing the primary inverter to operate at a fixed resonant frequency. Ultimately, both the waveform analysis and closed-loop simulations confirm that this architecture sustains reliable, efficient power delivery, proving its viability for practical wireless charging applications.

References

[1] K. A. Kalwar, M. Aamir, and S. Mekhilef, “Inductively Coupled Power Transfer (ICPT) for Electric Vehicle Charging—A Review,” Renewable and Sustainable Energy Reviews, vol. 47, pp. 462–475, 2015.

[2] D. A. G. Pedder, A. D. Brown, and J. A. Skinner, “A Contactless Electrical Energy Transmission System,” IEEE Transactions on Industrial Electronics, vol. 46, pp. 23–30, 1999.

[3] K. Aditya and S. S. Williamson, “Design Considerations for Loosely Coupled Inductive Power Transfer (IPT) System for Electric Vehicle Battery Charging—A Comprehensive Review,” in Proceedings of the IEEE Transportation Electrification Conference and Expo (ITEC), Dearborn, MI, USA, 15–18 June 2014.

[4] H. H. Wu, A. Gilchrist, K. D. Sealy, and D. Bronson, “A High Efficiency 5 kW Inductive Charger for EVs Using Dual Side Control,” IEEE Transactions on Industrial Informatics, vol. 8, pp. 585–595, 2012.

[5] A. W. Green and J. T. Boys, “10 kHz Inductively Coupled Power Transfer—Concept and Control,” in Proceedings of the Fifth International Conference on Power Electronics and Variable-Speed Drives, London, UK, 26–28 October 1994.

[6] G. A. Covic and J. T. Boys, “Inductive Power Transfer,” Proceedings of the IEEE, vol. 101, pp. 1276–1289, 2013.

[7] T. Diekhans and R. W. De Doncker, “A Dual-Side Controlled Inductive Power Transfer System Optimized for Large Coupling Factor Variations and Partial Load,” IEEE Transactions on Power Electronics, vol. 30, pp. 6320–6328, 2015.
[8] K. Sun and W. Niu, “SPWM Inverter Control for Wireless Constant Current and Voltage Charging,” World Electric Vehicle Journal, vol. 14, p. 111, 2023.
[9] T. Kan, T. D. Nguyen, J. C. White, R. K. Malhan, and C. C. Mi, “A New Integration Method for an Electric Vehicle Wireless Charging System Using LCC Compensation Topology: Analysis and Design,” IEEE Transactions on Power Electronics, vol. 32, pp. 1638–1650, 2017.
[10] F. Y. Lin, A. Zaheer, M. Budhia, and G. A. Covic, “Reducing Leakage Flux in IPT Systems by Modifying Pad Ferrite Structures,” in Proceedings of the 2014 IEEE Energy Conversion Congress and Exposition (ECCE), Pittsburgh, PA, USA, 14–18 September 2014.
[11] P. Zhang, Q. Yang, X. Zhang, Y. Li, and Y. Li, “Comparative Study of Metal Obstacle Variations in Disturbing Wireless Power Transmission System,” IEEE Transactions on Magnetics, vol. 53, pp. 1–4, 2017.
[12] X. Zhang, X. Ni, Q. Yang, B. Wei, and S. Wang, “Analysis of Electromagnetic Force on Metal Objects in Vertical Direction of Wireless Power Transfer,” in Proceedings of the 2019 IEEE PELS Workshop on Emerging Technologies: Wireless Power Transfer (WoW), London, UK, 18–21 June 2019.
[13] N. Bekiroglu, A. Agcal, and S. Ozcira, “Validation of Wireless Power Transfer by Using 3D Representation of Magnetically Coupled Resonators Considering Peak Efficiency,” Journal of Magnetics, vol. 23, pp. 11–17, 2018.
[14] S. Lee, G. Jung, S. Shin, Y. Kim, B. Song, J. Shin, and D. Cho, “The Optimal Design of High-Powered Power Supply Modules for Wireless Power Transferred Train,” in Proceedings of the 2012 Electrical Systems for Aircraft, Railway and Ship Propulsion, Bologna, Italy, 16–18 October 2012.
[15] A. Agcal, N. Bekiroglu, and S. Ozcira, “Comparison of Magnetic Resonant Coupling Wireless Power Transfer Systems within Aligned and Unaligned Positions and Determining Their Limits,” Journal of Magnetics, vol. 21, pp. 652–659, 2016.
[16] K. Aditya, “Design and Characteristics of Series–Series and Series–Parallel Topologies Fed from Constant-Voltage Fixed-Frequency Supply,” Sādhanā, vol. 42, pp. 163–171, 2017.
[17] M. Budhia, J. T. Boys, G. A. Covic, and C. Y. Huang, “Development of a Single-Sided Flux Magnetic Coupler for Electric Vehicle IPT Charging Systems,” IEEE Transactions on Industrial Electronics, vol. 60, pp. 318–328, 2013.
[18] U. Hentschel, M. Helwig, A. Winkler, and N. Modler, “Simulation of Foreign Object Detection Using Passive Inductive Sensors in a Wireless Charging System for Electric Vehicles,” World Electric Vehicle Journal, vol. 14, p. 241, 2023.
[19] C. Liu, C. Jiang, and C. Qiu, “Overview of Coil Designs for Wireless Charging of Electric Vehicle,” in Proceedings of the 2017 IEEE PELS Workshop on Emerging Technologies: Wireless Power Transfer (WoW), Chongqing, China, 20–22 May 2017.
[20] J. Sallán, J. L. Villa, A. Llombart, and J. F. Sanz, “Optimal Design of ICPT Systems Applied to Electric Vehicle Battery Charge,” IEEE Transactions on Industrial Electronics, vol. 56, pp. 2140–2149, 2009.